



SAR and molecular mechanism study of novel acylhydrazone compounds targeting HIV-1 CA

Yinxue Jin^a, Zhiwu Tan^a, Meizi He^a, Baohe Tian^a, Shixing Tang^b, Indira Hewlett^b, Ming Yang^{a,*}

^aState Key Laboratory of Natural and Biomimetic Drugs, Peking University, PO Box 261, Beijing 100191, China

^bCenter for Biologics Evaluation and Research, Food and Drug Administration, Bethesda, MD 20892, USA

ARTICLE INFO

Article history:

Received 12 December 2009

Revised 30 January 2010

Accepted 2 February 2010

Available online 6 February 2010

Keywords:

HIV-1

Capsid assembly

Antiviral

Acylhydrazone derivatives

ABSTRACT

We synthesized a series of acylhydrazone compounds bearing naturally occurring amino acids' side chains as HIV assembly inhibitors. Biological evaluation indicated that the compounds had anti-SIV and capsid assembly inhibitory activities. The structure–activity relationship (SAR) study showed that compounds bearing proper aromatic side chains had potential antiviral activities. The molecular modeling experiments revealed the molecular mechanism that they could bind to CA in the same manner as CAP-1 and occupy two more grooves.

© 2010 Published by Elsevier Ltd.

1. Introduction

In the past few years, scientists have made dramatic efforts to develop new targets of human immunodeficiency virus (HIV) and their inhibitors. Recent studies have revealed that HIV-1 capsid proteins can assemble into a cone-shaped structure encapsidating the viral nucleocapsid/RNA genome complex which performs essential function for efficient replication.^{1,2} Mutations in CA that inhibit assembly are lethal, and mutations that alter capsid stability severely attenuate replication, making the capsid protein an attractive target.³

In our previous work we had found that acylhydrazone derivatives containing naturally occurring amino acid moiety had good anti-SIV activities and focused on compounds containing a L-phenylalanine side chain which showed great potential (see Fig. 1).⁴ This paper is aimed to find more potent compounds by introducing different naturally occurring amino acid side chains to the acylhydrazone compounds so as to further investigate the structure–activity relationship (SAR) and molecular mechanism of this class of acylhydrazone compounds. In our previous work, we had found that compounds bearing electro-donating group at *p*-position of the left phenyl ring had good antiviral activities.⁴ Hence to study the SAR more efficiently and reasonably, we kept the left ring substituted with *p*-methoxyl group and performed the following modifications: (1) We introduced different naturally occurring amino acids to the acylhydrazone compounds. (2) We substituted

the *p*-position of the right phenyl ring with electron-donating, electron-withdrawing and hydrophobic groups, or replaced the right phenyl ring with heterocyclic ring. Based on the above strategy, we obtained a series of novel acylhydrazone derivatives and evaluated their antiviral activities and assembly inhibitory activities. We also performed molecular modeling experiments with our compounds to gain more insight into the molecular mechanism.

2. Results and discussion

The route used for preparation of the title compounds is illustrated in Scheme 1 and the detailed synthetic procedure is explained in Section 4. Twenty-three compounds were obtained and their MS, ¹H NMR spectroscopy data are provided in Section 4. According to the literature, this array of acylhydrazone compounds are in form of *E* geometrical isomer for C=N double bond in DMSO-*d*₆, and the *E* geometrical isomer undergoes a rapid *cis/trans* amide equilibrium at room temperature.^{5,6} Analytic results of the ¹H NMR spectra of our synthesized compounds answered for the literature.

We tested the concentration for 50% of maximum effect (EC₅₀), concentration for 50% of maximum toxic (TC₅₀) and therapeutic index (TI = TC₅₀/EC₅₀) values of our title compounds using SIV-induced syncytium assay in CEM cells. The results are summarized in Table 1.

As shown in Table 1, each of the title compounds exhibited an EC₅₀ value within the range from 0.41 μM to 14.86 μM while most of them possessed a TC₅₀ value more than 100, indicating that all

* Corresponding author. Tel.: +86 10 82805264; fax: +86 10 82802724.

E-mail address: yangm@bjmu.edu.cn (M. Yang).

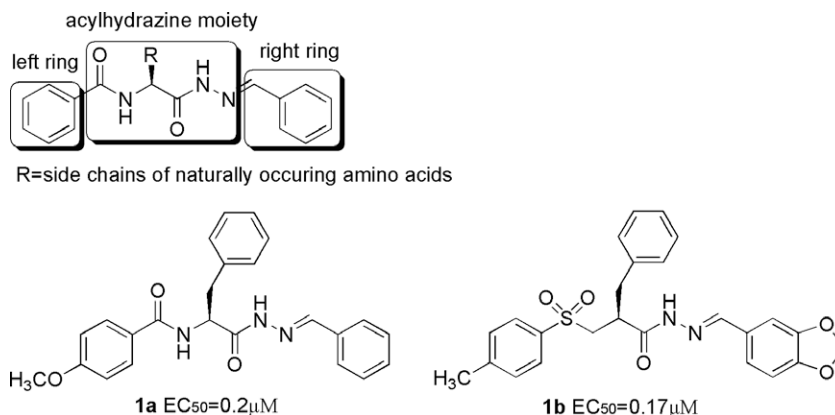


Figure 1. The structure of acylhydrazone compounds containing amino acid moiety.

compounds had effective anti-SIV activities while most of them had low cytotoxicities.

In our preliminary study, compounds **5a–d** and **5e–k** were synthesized to investigate the SAR of the side chains moiety and the right ring portion. By taking a detailed look in Table 1, we found that: (1) Compounds bearing alkane side chain (**5a–d**) all exhibited good anti-SIV activities, of which the compound bearing a hydroxyl alkane side chain performed better activity (**5d** versus **5a–c**), giving us a hint that hydrogen bond at the side chains might benefit inhibitory activities. (2) Substituent changes of the right phenyl ring had little influence on anti-SIV activity (**5e–g** versus **5c**, **5i–k** vs **5d**). (3) Replacement of the right phenyl ring with a furan ring led to better activity when the side chains were alkane chain (**5h** vs **5c**). Our previous work had found that acylhydrazone derivatives containing a α -phenylalanine moiety at the side chain possessed good anti-SIV activities and the phenyl ring of the side chain functioned by occupying a groove.⁴ Therefore, we designed compounds bearing side chain of α -tyrosine which had both phenyl ring and hydroxyl group, and synthesized compounds **6a–e**. They possessed fair anti-SIV activity not as good as acylhydrazone derivatives bearing an α -phenylalanine side chain, and displayed high cytotoxicities. Maybe it was the hydrogen bond interaction between the hydroxyl group and the capsid protein that hindered the phenyl ring from fitting into the groove. Taking all the above factors into account, we chose small α -histidine to design the side chain. The imidazole ring of α -histidine was not only an aromatic ring, but also a hydrogen bond donor and receptor. Finally we synthesized **8a–g**. As we expected, all of them exhibited significant anti-SIV activity, especially **8a** and **8b**, with an EC_{50} value of 0.56 μ M and 0.41 μ M, respectively. However, there was no significant difference between the EC_{50} values of **8a** and **8b** and the EC_{50} values of **1a** and **1b** (EC_{50} = 0.2 μ M and 0.17 μ M).

To ascertain that the compounds could target HIV-1 CA, we performed ultraviolet spectrophotometry analysis to measure sample turbidity caused by capsid assemble protein.^{3,7} In our study this

assay was used to probe for potential inhibitory effects of the acylhydrazone derivatives on in vitro capsid assembly. CAP-1, a well-known capsid assembly inhibitor, was used as a reference compound in this assay. The results are summarized in Table 2.

According to Table 2, dissolution of native HIV-CA into assembly buffer led to an increase in absorbance at an initial rate of 60.56 mOD/min, while in the presence of CAP-1 the initial assembly rate decreased to 31.37 mOD/min. In the presence of each title compound, the capsid assembly rate performed a value ranging from 3.26 mOD/min to 49.45 mOD/min, suggesting that all compounds could inhibit capsid assembly effectively.

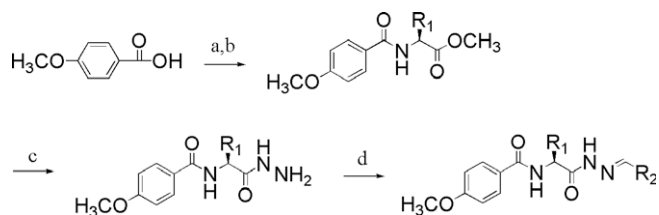
Especially as shown in Figure 2, we found that in the presence of compounds **8a** and **8b** which showed high activities, the turbidity value decreased significantly. Meanwhile, in the presence of compounds **5e** and **6c** which showed low activities, the turbidity value slightly decreased. The results demonstrated that **8a** and **8b** could inhibit capsid assembly more efficiently than **5e** and **6c**, reflecting that the antiviral activity was corresponding to the ability to inhibit capsid assembly.

As mentioned before, the EC_{50} values of our compounds **8a** and **8b** (0.56 μ M and 0.41 μ M) were basically at the same level as the EC_{50} value of compounds **1a** and **1b** (0.2 μ M and 0.17 μ M). However, the capsid assembly rate values in presence of **8a** and **8b** (3.26 ± 1.03 mOD/min and 3.58 ± 0.25 mOD/min) were significantly lower than those of **1a** and **1b** (22.6 ± 0.6 mOD/min and 7.9 ± 0.6 mOD/min),⁴ suggesting that compounds **8a** and **8b** could inhibit capsid assembly more effectively than compounds **1a** and **1b**.

To further study the molecular mechanism of these novel acylhydrazone compounds, we performed molecular modeling experiments using the program AUTODOCK 4.0. The free binding energies of our tested compounds and CAP-1 are listed in Table 3.

As shown in Table 3, all of our tested compounds exhibited free energies below -9 kcal/mol and most of them possessed free energy lower than that of CAP-1, confirming that the compounds could bind to CA. Seeing through Table 3, we found that: (1) Compounds bearing alkane side chains had close free energies (**5a–d**). (2) Compounds bearing aromatic side chains (**8a–b**) displayed noticeable low free energies, except that compound **6a** showed relatively high free energy. (3) The free energies of our tested compounds were in agreement with their assembly rate values, as **8a** and **8b** with assembly rate values of 3.26 mOD/min and 3.58 mOD/min exhibited free energies of -12.73 kcal/mol and -12.78 kcal/mol while **5e** and **5g** with assembly rate values of 33.38 mOD/min and 30.08 mOD/min exhibited free energies of -9.35 kcal/mol and -9.57 kcal/mol.

The binding models of our tested compounds showed that: (1) The right ring inserted into the pocket vacated by Phe 32 in the



Scheme 1. Reagents and conditions: (a) $SOCl_2$, $CHCl_3$, reflux, 6 h; (b) L-amino acid methyl ester hydrochloride, Et_3N , CH_2Cl_2 , $0^\circ C$ to rt, 5 h; (c) 85% $NH_2NH_2 \cdot H_2O$, CH_3CH_2OH , reflux, 6–8 h; (d) R_2-CHO , anhydrous CH_3OH , rt, 1–2 h.

Table 1
Inhibition effects and cytotoxicities of the title compounds on SIV-induced syncytium

Entry	R ₁	R ₂	TC ₅₀	EC ₅₀	TI
5a	-CH ₃	-C ₆ H ₅	>100	6.41	>15.60
5b	-CH(CH ₃) ₂	-C ₆ H ₅	>100	4.08	>24.51
5c	-CH(CH ₃)CH ₂ CH ₃	-C ₆ H ₅	77.87	7.65	10.18
5d	-CH(CH ₃)OH	-C ₆ H ₅	>100	0.77	>129.87
5e	-CH(CH ₃)CH ₂ CH ₃	-C ₆ H ₄ -CH ₃	>100	13.89	>7.20
5f	-CH(CH ₃)CH ₂ CH ₃	-C ₆ H ₄ -Cl	>100	8.10	>12.35
5g	-CH(CH ₃)CH ₂ CH ₃	-C ₆ H ₄ -OH	>100	4.15	>24.10
5h	-CH(CH ₃)CH ₂ CH ₃	-C ₅ H ₄ O	>100	1.70	>58.82
5i	-CH(CH ₃)OH	-C ₆ H ₄ -CH ₃	>100	8.17	>12.24
5j	-CH(CH ₃)OH	-C ₆ H ₄ -Cl	>100	4.98	>20.08
5k	-CH(CH ₃)OH	-C ₆ H ₄ -OH	>100	8.13	>12.30
6a	-C ₆ H ₄ -OH	-C ₆ H ₅	>100	4.61	>21.69
6b	-C ₆ H ₄ -OH	-C ₆ H ₄ -CH ₃	41.15	5.21	7.90
6c	-C ₆ H ₄ -OH	-C ₆ H ₄ -Cl	39.96	14.86	2.69
6d	-C ₆ H ₄ -OH	-C ₆ H ₄ -OH	>100	7.81	>12.80
6e	-C ₆ H ₄ -OH	-C ₅ H ₄ O	30.56	9.03	3.38
8a	-C ₄ H ₃ NH	-C ₆ H ₅	>100	0.56	>178.57
8b	-C ₄ H ₃ NH	-C ₆ H ₄ -OCH ₃	>100	0.41	>243.90
8c	-C ₄ H ₃ NH	-C ₆ H ₄ -CH ₃	>100	1.55	64.52
8d	-C ₄ H ₃ NH	-C ₆ H ₄ -NO ₂	>100	4.40	>22.73
8e	-C ₄ H ₃ NH	-C ₆ H ₄ -Cl	>100	3.27	>30.58
8f	-C ₄ H ₃ NH	-C ₆ H ₄ -OH	>100	3.18	>31.45
8g	-C ₄ H ₃ NH	-C ₅ H ₄ O	>100	8.44	>11.85

same manner as CAP-1. (2) The left ring occupied a hydrophobic groove surrounded by Val24, Val27, Thr58 and Val59. (3) The alkane side chains appeared generally disordered while the aromatic side chains occupied a groove surrounded by Val26, Val29, Ala31 and Phe32, except that the aromatic side chains with hydrogen bond donor could form hydrogen bond with the backbone oxygen of Glu28. As typical compounds, the stereo views of compounds **5c**, **5d**, **6a** and **8a** are illustrated in Figure 3.

Looking at Figure 3, we found that: (1) Compounds **5c** and **5d** shared the exact model we described above and no hydrogen bond was formed. (2) The imidazole ring of **8a** could fit well into the groove we mentioned above while the phenyl ring of **6a** was hindered by hydrogen bond just as we assumed before. All the above

Table 2
Assembly inhibitory data of acylhydrazone derivatives

Entry	Assembly rate ^a (mOD/min)
CA	60.56 ± 3.77
CAP-1	31.37 ± 1.16
5c	25.44 ± 0.84
5d	21.45 ± 1.08
5e	33.38 ± 0.76
5f	10.23 ± 1.54
5g	30.08 ± 0.39
5h	5.82 ± 0.37
5i	11.88 ± 0.47
5j	49.45 ± 2.34
5k	24.88 ± 0.56
6a	32.53 ± 2.07
6b	20.41 ± 0.68
6c	24.26 ± 0.42
6d	8.77 ± 0.19
6e	19.05 ± 0.35
8a	3.26 ± 1.03
8b	3.58 ± 0.25
8c	6.05 ± 0.16
8d	12.59 ± 0.27
8e	8.89 ± 0.18
8f	24.66 ± 0.40
8g	29.32 ± 0.47

^a Each value is reported as the mean ± SD (standard deviation) from two experiments in duplicate.

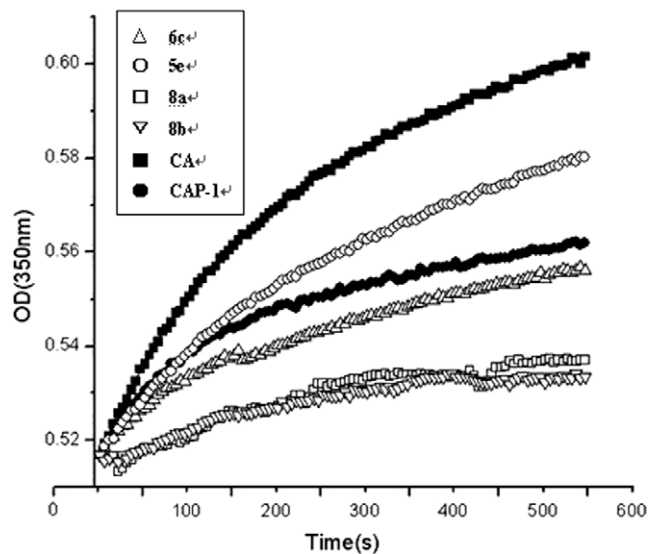


Figure 2. Turbidity assay results showing the effects of CA-binding compounds on in vitro capsid assembly

Table 3
Free binding energies

Entry	Free energy (kal/mol)
CAP-1	-10.58
5a	-10.79
5b	-11.23
5c	-10.95
5d	-10.64
5e	-9.35
5g	-9.57
5j	-10.06
6a	-10.88
8a	-12.73
8b	-12.78

results were in agreement with the results obtained from Table 3. And the stereo view of **8a** to capsid protein was the same as that of

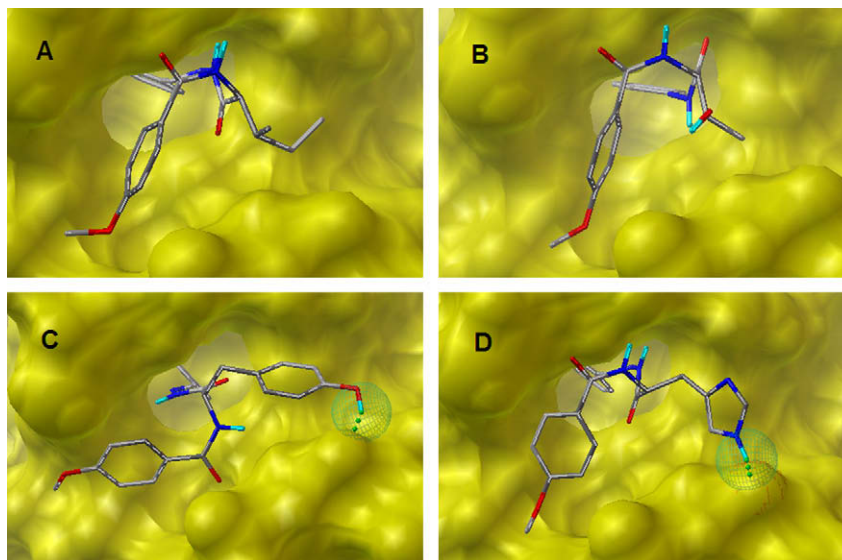


Figure 3. (A) Stereo view of **5c** to capsid protein; (B) stereo view of **5d** to capsid protein; (C) stereo view of **6a** to capsid protein; (D) stereo view of **8a** to capsid protein. The hydrogen bond is highlighted with green dots.

the binding model of compound **1b**.⁴ Based on the facts that compounds **8a–b** and **1a–b** had good antiviral activities, we could reach the conclusion that the side chain occupying a groove was an important mechanism of these acylhydrazone molecules, giving clues for further study.

3. Conclusion

In this work, all experiments reported here showed that the newly designed acylhydrazone compounds could inhibit capsid assembly and had potent inhibitory activities of SIV. The SAR study revealed that the introduction of proper aromatic side chains could enhance inhibitory activities significantly. Molecular modeling experiments confirmed the molecular mechanism that compounds bearing proper aromatic side chains could bind to capsid protein in the same manner as CAP-1 and occupy two other hydrophobic grooves. Compounds bearing an L-histidine side chain had good antiviral activities, of which compound **8a** and **8b** exhibited the most promising activities with EC₅₀ values of 0.56 μM and 0.41 μM and TI values of above 179 and 244, respectively.

4. Experimental

4.1. Chemistry

All materials were commercially available and used without further purification. All the titled compounds were characterized by ¹H NMR spectra on a Varian 300 MHz or Bruke AM-300 spectrometer using the solvents described. Chemical shifts were reported in δ ppm (parts per million) relative to tetramethyl silane (TMS) except for deuterated water (D₂O) and the signals were quoted as s (singlet), d (doublet), t (triplet), q (quartet), and m (multiplet). The mass spectra (EI or ESI) were recorded. Melting points were determined on an XA-4 instrument which was uncorrected.

4.2. General synthetic procedure

Starting from natural occurring amino acids, they were first converted to their corresponding *N*-(4-methoxybenzoyl) amino acid methyl esters by reaction with thionyl chloride in methanol,⁸

followed by addition of 4-methoxybenzoyl chloride in the presence of triethylamine in chloroform.⁹ The appropriate *N*-(4-methoxybenzoyl) amino acid methyl ester (20 mmol) was added in small portions to a stirred solution of 85% hydrazine hydrate (5 mL) in ethanol (10 mL). The mixture was heated under reflux for 6–8 h. After being cooled to room temperature, the resulting precipitate was filtered in vacuo, washed with cold water and dried to give the corresponding acylhydrazine. To a magnetically suspension of the above acylhydrazine (0.5 mmol) in anhydrous methanol (2 mL) was added substituted benzaldehyde (0.5 mmol). Shortly the solution became homogeneous (heating could promote this process) and within minutes the resulting hydrazone began to precipitate. After the mixture was stirred for further 1–2 h at room temperature, the precipitate was collected by filtration, washed with a small quantity of cold methanol and dried. Recrystallization of the reaction product from methanol gave the pure hydrazone.

4.2.1. (*S,E*)-*N*-(1-(2-Benzylidenehydrazinyl)-1-oxopropan-2-yl)-4-methoxybenzamide (**5a**)

Compound **5a** was white solid, mp 182–183 °C, yield 82.8%. ¹H NMR (DMSO-*d*₆) δ 1.39–1.43 (dd, 3H, *J* = 7.5 Hz), 3.81 (s, 3H), 4.50, 5.31 (2 m, 1H), 6.98–7.01 (d, 2H), 7.43 (m, 3H), 7.68 (m, 2H), 7.89–7.92 (d, 2H), 8.01, 8.25 (2s, 1H), 8.43–8.53 (2d, 1H), 11.37, 11.54 (2s, 1H); MS (ESI⁺) *m/z* calcd: 325.14, found: 324.0 [(*M*–1)⁺].

4.2.2. (*S,E*)-*N*-(1-(2-Benzylidenehydrazinyl)-3-methyl-1-oxobutan-2-yl)-4-methoxybenzamide (**5b**)

Compound **5b** was white solid, mp 224–225 °C, yield 53.5%. ¹H NMR (DMSO-*d*₆) δ 0.93–1.01 (m, 6H), 2.18–2.27 (m, 1H), 3.81 (s, 3H), 4.27, 5.37 (2 m, 1H), 6.97–7.01 (2d, 2H), 7.43–7.46 (m, 3H), 7.68–7.71 (m, 2H), 7.88–7.92 (m, 2H), 8.00, 8.25 (2s, 1H), 8.12, 8.40 (2d, 1H), 11.47, 11.67 (2s, 1H); MS (ESI⁺) *m/z* calcd: 353.17, found: 352.2 [(*M*–1)⁺].

4.2.3. *N*-((2*S*,3*R*)-1-((*E*)-2-Benzylidenehydrazinyl)-3-methyl-1-oxopentan-2-yl)-4-methoxybenzamide (**5c**)

Compound **5c** was white solid, mp 241–242 °C, yield 84.9%. ¹H NMR (DMSO-*d*₆) δ 0.84–0.95 (m, 6H), 1.24, 1.57 (2 m, 2H), 2.04 (m, 1H), 3.81 (s, 3H), 4.33, 5.45 (2t, 1H), 6.97–7.01 (2d, 2H, *J* = 3), 7.43–7.46 (m, 3H), 7.68–7.71 (m, 2H), 7.87–7.92 (m, 2H), 8.00, 8.25 (2s, 1H), 8.16, 8.43 (2d, 1H), 11.46, 11.69 (2s, 1H); ESI-MS: *m/z* calcd: 367.19, found: 366.3 [(*M*–1)⁺].

4.2.4. *N*-((2*S*,3*R*)-1-((*E*)-2-Benzylidenehydrazinyl)-3-hydroxy-1-oxobutan-2-yl)-4-methoxybenzamide (5d)

Compound **5d** was white solid, mp 160–161 °C, yield 85.0%. ¹H NMR (DMSO-*d*₆) δ 1.13–1.21 (2d, 3H, *J* = 6.0 Hz), 3.83 (s, 3H), 4.12, 4.24 (2 m, 1H), 4.43, 5.33 (2q, 1H), 4.86, 5.03 (2d, 1H), 7.02–7.05 (d, 2H), 7.42–7.50 (m, 3H), 7.68–7.70 (m, 2H), 7.87–7.92 (m, 2H), 7.80, 7.98 (2d, 1H), 8.02, 8.26 (2s, 1H), 11.46–11.49 (d, 1H); ESI-MS: *m/z* calcd: 355.15, found: 354.4 [(*M*–1)⁺].

4.2.5. 4-Methoxy-*N*-((2*S*,3*R*)-3-methyl-1-((*E*)-2-(4-methylbenzylidene)hydrazinyl)-1-oxopentan-2-yl)benzamide (5e)

Compound **5e** was white solid, mp 235 °C, yield 87.6%. ¹H NMR (DMSO-*d*₆) δ 0.84–0.94 (m, 6H), 1.24, 1.56 (2 m, 2H), 2.01 (m, 1H), 3.81 (s, 3H), 4.32, 5.44 (2t, 1H), 6.98–7.01 (d, 2H), 7.24–7.27 (d, 2H), 7.57–7.60 (d, 2H), 7.89–7.92 (d, 2H), 7.97, 8.20 (2s, 1H), 8.15, 8.42 (2d, 1H), 11.40, 11.63 (2s, 1H); ESI-MS: *m/z* calcd: 381.21, found: 380.2 [(*M*–1)⁺].

4.2.6. *N*-((2*S*,3*R*)-1-((*E*)-2-(4-Chlorobenzylidene)hydrazinyl)-3-methyl-1-oxopentan-2-yl)-4-methoxybenzamide (5f)

Compound **5f** was white solid, mp 215–216 °C, yield 92.3%. ¹H NMR (DMSO-*d*₆) δ 0.84–0.94 (m, 6H), 1.23, 1.57 (2 m, 2H), 2.02 (m, 1H), 3.81 (s, 3H), 4.32, 5.42 (2t, 1H), 6.97–7.01 (2d, 2H), 7.50–7.53 (d, 2H), 7.71–7.74 (d, 2H), 7.89–7.93 (2d, 2H), 7.99, 8.24 (2s, 1H), 8.21, 8.46 (2d, 1H), 11.54, 11.79 (2s, 1H); ESI-MS: *m/z* calcd: 401.15, found: 400.2 [(*M*–1)⁺].

4.2.7. *N*-((2*S*,3*R*)-1-((*E*)-2-(4-Chlorobenzylidene)hydrazinyl)-3-methyl-1-oxopentan-2-yl)-4-methoxybenzamide (5g)

Compound **5g** was white solid, mp 144–146 °C, yield 93.5%. ¹H NMR (DMSO-*d*₆) δ 0.86–0.94 (m, 6H), 1.24, 1.56 (2 m, 2H), 2.03 (m, 1H), 3.81 (s, 3H), 4.30, 5.42 (2t, 1H), 6.80–6.85 (dd, 2H), 6.98–7.01 (d, 2H), 7.50–7.53 (d, 2H), 7.66–7.91 (dd, 2H), 8.13 (s, 1H), 8.40–8.43 (d, 1H), 11.27, 11.49 (2s, 1H); ESI-MS: *m/z* calcd: 383.18, found: 382.3 [(*M*–1)⁺].

4.2.8. *N*-((2*S*,3*R*)-1-((*E*)-2-(4-Chlorobenzylidene)hydrazinyl)-3-methyl-1-oxopentan-2-yl)-4-methoxybenzamide (5h)

Compound **5h** was pale brown solid, mp 220–221 °C, yield 81.2%. ¹H NMR (DMSO-*d*₆) δ 0.83–0.93 (m, 6H), 1.24, 1.55 (2 m, 2H), 2.00 (m, 1H), 3.81 (s, 3H), 4.30, 5.34 (2t, 1H), 6.62–6.64 (m, 1H), 6.87–6.91 (2d, 1H), 6.98–7.01 (d, 2H), 7.83–7.92 (m, 3H), 8.13 (s, 1H), 8.43–8.46 (d, 1H), 11.41, 11.65 (2s, 1H); ESI-MS: *m/z* calcd: 357.17, found: 356.2 [(*M*–1)⁺].

4.2.9. *N*-((2*S*,3*R*)-1-((*E*)-2-Benzylidenehydrazinyl)-3-hydroxy-1-oxobutan-2-yl)-4-methoxybenzamide (5i)

Compound **5i** was white solid, mp 155–156 °C, yield 89.6%. ¹H NMR (DMSO-*d*₆) δ 1.13–1.20 (2d, 3H, *J* = 6.0 Hz), 2.34 (s, 3H), 3.83 (s, 3H), 4.11, 4.22 (2 m, 1H), 4.42, 5.32 (2q, 1H), 4.88, 5.04 (2d, 1H), 7.03–7.05 (d, 2H), 7.24–7.29 (dd, 2H), 7.57–7.59 (d, 2H), 7.87–7.93 (dd, 2H), 7.83, 8.03 (2d, 1H), 7.98, 8.21 (2s, 1H), 11.43–11.47 (d, 1H); ESI-MS: *m/z* calcd: 369.17, found: 368.1 [(*M*–1)⁺].

4.2.10. *N*-((2*S*,3*R*)-1-((*E*)-2-(4-Chlorobenzylidene)hydrazinyl)-3-hydroxy-1-oxobutan-2-yl)-4-methoxybenzamide (5j)

Compound **5j** was white solid, mp 168–170 °C, yield 90.3%. ¹H NMR (DMSO-*d*₆) δ 1.13–1.20 (2d, 3H, *J* = 6.3 Hz), 3.83 (s, 3H), 4.12, 4.20 (2 m, 1H), 4.43, 5.32 (2q, 1H), 4.88–5.08 (2d, 1H), 7.03–7.05 (d, 2H), 7.50–7.55 (dd, 2H), 7.71–7.73 (d, 2H), 7.88–7.93 (dd, 2H), 8.01, 8.25 (2s, 1H), 8.05–8.08 (d, 1H), 11.57–11.63 (d, 1H); ESI-MS: *m/z* calcd: 389.11, found: 388.0 [(*M*–1)⁺].

4.2.11. *N*-((2*S*,3*R*)-3-Hydroxy-1-((*E*)-2-(4-hydroxybenzylidene)hydrazinyl)-1-oxobutan-2-yl)-4-methoxybenzamide (5k)

Compound **5k** was pale white solid, mp 133–134 °C, yield 93.4%. ¹H NMR (DMSO-*d*₆) δ 1.12–1.20 (2d, 3H, *J* = 6.0 Hz), 3.83 (s, 3H), 4.12, 4.24 (2 m, 1H), 4.41, 5.30 (2q, 1H), 4.86, 5.03 (2d, 1H), 6.80–6.85 (dd, 2H), 7.03–7.06 (d, 2H), 7.50–7.53 (d, 2H), 7.87–7.92 (dd, 2H), 8.00–8.03 (d, 1H), 8.13 (s, 1H), 9.79, 9.96 (2s, 1H), 11.29–11.33 (d, 1H); ESI-MS: *m/z* calcd: 371.15, found: 370.1 [(*M*–1)⁺].

4.2.12. (*S*,*E*)-*N*-(1-(2-Benzylidenehydrazinyl)-3-(4-hydroxyphenyl)-1-oxopropan-2-yl)-4-methoxybenzamide (6a)

Compound **6a** was white solid, mp 185–186 °C, yield 50.0%. ¹H NMR (DMSO-*d*₆) δ 2.97–2.99 (d, 2H), 3.81 (s, 3H), 4.64, 5.47 (2 m, 1H), 6.65–6.68 (d, 2H), 6.98–7.01 (d, 2H), 7.17–7.20 (d, 2H), 7.44–7.50 (m, 2H), 7.70–7.75 (m, 2H), 7.83–7.86 (d, 2H), 8.05, 8.24 (2s, 1H), 8.49–8.63 (2d, 1H), 9.21 (s, 1H), 11.47, 11.70 (2s, 1H); EI-MS: *m/z* calcd: 417.17, found: 417.

4.2.13. (*S*,*E*)-*N*-(3-(4-Hydroxyphenyl)-1-(2-(4-methylbenzylidene)hydrazinyl)-1-oxopropan-2-yl)-4-methoxybenzamide (6b)

Compound **6b** was white solid, mp 201–202 °C, yield 86.9%. ¹H NMR (DMSO-*d*₆) δ 2.43, 2.44 (2s, 3H), 2.96–2.98 (d, 2H), 3.81 (s, 3H), 4.63, 5.46 (2 m, 1H), 6.64–6.67 (m, 2H), 6.98–7.01 (d, 2H), 7.15–7.18 (d, 2H), 7.25–7.32 (2d, 2H), 7.58–7.64 (dd, 2H), 7.82–7.85 (d, 2H), 8.00, 8.19 (2s, 1H), 8.47–8.61 (2d, 1H), 9.20 (s, 1H), 11.39, 11.62 (2s, 1H); ESI-MS: *m/z* calcd: 431.18, found: 430.2 [(*M*–1)⁺].

4.2.14. (*S*,*E*)-*N*-(1-(2-(4-Chlorobenzylidene)hydrazinyl)-3-(4-hydroxyphenyl)-1-oxopropan-2-yl)-4-methoxybenzamide (6c)

Compound **6c** was white solid, mp 197–199 °C, yield 90.1%. ¹H NMR (DMSO-*d*₆) δ 2.98 (s, 2H), 3.81 (s, 3H), 4.62, 5.47 (2 m, 1H), 6.66 (m, 2H), 6.98–7.00 (m, 2H), 7.20 (m, 2H), 7.54–7.57 (m, 2H), 7.73–7.84 (m, 4H), 8.01, 8.23 (2s, 1H), 8.50–8.61 (2d, 1H), 9.19 (s, 1H), 11.50, 11.74 (2s, 1H); ESI-MS: *m/z* calcd: 451.13, found: 450.2 [(*M*–1)⁺].

4.2.15. (*S*,*E*)-*N*-(1-(2-(4-Hydroxybenzylidene)hydrazinyl)-3-(4-hydroxyphenyl)-1-oxopropan-2-yl)-4-methoxybenzamide (6d)

Compound **6d** was white solid, mp 142–143 °C, yield 89.6%. ¹H NMR (DMSO-*d*₆) δ 2.94–2.96 (d, 2H), 3.80 (s, 3H), 4.61, 5.42 (2 m, 1H), 6.63–6.67 (2d, 2H), 6.80–6.88 (2d, 2H), 6.97–7.00 (d, 2H), 7.15–7.18 (2d, 2H), 7.51–7.58 (2d, 2H), 7.81–7.84 (d, 2H), 7.93, 8.11 (2s, 1H), 8.44–8.59 (2d, 1H), 9.20 (s, 1H), 9.94–9.96 (d, 1H), 11.26, 11.47 (2s, 1H); ESI-MS: *m/z* calcd: 433.16, found: 432.2 [(*M*–1)⁺].

4.2.16. (*S*,*E*)-*N*-(1-(2-(Furan-2-ylmethylene)hydrazinyl)-3-(4-hydroxyphenyl)-1-oxopropan-2-yl)-4-methoxybenzamide (6e)

Compound **6e** was brown solid, mp 134–136 °C, yield 78.3%. ¹H NMR (DMSO-*d*₆) δ 2.95–2.97 (d, 2H), 3.81 (s, 3H), 4.61, 5.33 (2 m, 1H), 6.63–6.68 (m, 3H), 6.91 (m, 1H), 6.98–7.01 (d, 2H), 7.13–7.25 (2d, 2H), 7.82–7.84 (d, 2H), 7.92–7.94 (d, 1H), 8.12 (s, 1H), 8.43–8.61 (2d, 1H), 9.19 (s, 1H), 11.41, 11.61 (2s, 1H); ESI-MS: *m/z* calcd: 407.15, found: 406.2 [(*M*–1)⁺].

4.2.17. (*S*,*E*)-*N*-(1-(2-Benzylidenehydrazinyl)-3-(1*H*-imidazol-4-yl)-1-oxopropan-2-yl)-4-methoxybenzamide (8a)

Compound **8a** was white solid, mp 203–204 °C, yield 73.7%. ¹H NMR (DMSO-*d*₆) δ 3.04 (s, 2H), 3.81 (s, 3H), 4.69, 5.53 (2 m, 1H), 6.87 (s, 1H), 7.00–7.03 (d, 2H), 7.43–7.45 (m, 3H), 7.57 (s, 1H), 7.66–7.76 (m, 2H), 7.83–7.87 (2d, 2H), 8.00, 8.25 (2s, 1H), 8.59–8.67 (m, 1H), 11.41, 11.60 (2s, 1H), 11.81 (s, 1H); ESI-MS: *m/z* calcd: 391.16, found: 392.0 [(*M*+1)⁺].

4.2.18. (S,E)-N-(3-(1H-Imidazol-4-yl)-1-(2-(4-methoxybenzylidene)hydrazinyl)-1-oxopropan-2-yl)-4-methoxybenzamide (8b)

Compound **8b** was white solid, mp 216–217 °C, yield 69.4%. ¹H NMR (DMSO-*d*₆) δ 3.03 (s, 2H), 3.80 (s, 6H), 4.67, 5.51 (2 m, 1H), 6.86 (s, 1H), 6.98–7.00 (d, 4H), 7.58–7.68 (m, 3H), 7.82–7.85 (m, 2H), 7.93, 8.16 (2s, 1H), 8.52–8.62 (2d, 1H), 11.25, 11.43 (2s, 1H); ESI-MS: *m/z* calcd: 421.18, found: 422.0 [(M+1)⁺].

4.2.19. (S,E)-N-(3-(1H-Imidazol-4-yl)-1-(2-(4-methylbenzylidene)hydrazinyl)-1-oxopropan-2-yl)-4-methoxybenzamide (8c)

Compound **8c** was white solid, mp 242–243 °C, yield 67.5%. ¹H NMR (DMSO-*d*₆) δ 2.34 (s, 3H), 3.04 (s, 2H), 3.81 (s, 3H), 4.68, 5.52 (2 m, 1H), 6.87 (s, 1H), 6.99–7.02 (d, 2H), 7.24–7.26 (d, 2H), 7.55–7.64 (m, 3H), 7.83–7.87 (m, 2H), 7.96, 8.20 (2s, 1H), 8.58–8.65 (m, 1H), 11.34, 11.53 (2s, 1H), 11.81 (s, 1H); ESI-MS: *m/z* calcd: 405.18, found: 406.0 [(M+1)⁺].

4.2.20. (S,E)-N-(3-(1H-Imidazol-4-yl)-1-(2-(4-nitrobenzylidene)hydrazinyl)-1-oxopropan-2-yl)-4-methoxybenzamide (8d)

Compound **8d** was yellow solid, mp 236–237 °C, yield 69.7%. ¹H NMR (DMSO-*d*₆) δ 3.05 (s, 2H), 3.81 (s, 3H), 4.70, 5.56 (2 m, 1H), 6.92 (s, 1H), 7.00–7.02 (d, 2H), 7.58 (s, 1H), 7.84–7.87 (m, 2H), 7.93–7.95 (d, 1H), 8.03–8.04 (d, 1H), 8.09, 8.36 (2s, 1H), 8.27–8.30 (2d, 1H), 11.68, 11.80, 11.90 (3s, 2H); ESI-MS: *m/z* calcd: 436.15, found: 437.0 [(M+1)⁺].

4.2.21. (S,E)-N-(1-(2-(4-Chlorobenzylidene)hydrazinyl)-3-(1H-imidazol-4-yl)-1-oxopropan-2-yl)-4-methoxybenzamide (8e)

Compound **8e** was yellow solid, mp 248–249 °C, yield 82.8%. ¹H NMR (DMSO-*d*₆) δ 3.04 (s, 2H), 3.81 (s, 3H), 4.69, 5.53 (2 m, 1H), 6.88 (s, 1H), 7.00–7.02 (d, 2H), 7.49–7.51 (d, 2H), 7.56 (s, 1H), 7.69–7.71 (d, 1H), 7.76–7.78 (d, 1H), 7.83–7.86 (m, 2H), 7.98, 8.24 (2s, 1H), 8.63 (m, 1H), 11.43, 11.64, 11.79 (3s, 2H); ESI-MS: *m/z* calcd: 425.13, found: 426.0 [(M+1)⁺].

4.2.22. (S,E)-N-(1-(2-(4-Hydroxybenzylidene)hydrazinyl)-3-(1H-imidazol-4-yl)-1-oxopropan-2-yl)-4-methoxybenzamide (8f)

Compound **8f** was white solid, mp 162–163 °C, yield 66.8%. ¹H NMR (DMSO-*d*₆) δ 3.04 (s, 2H), 3.81 (s, 3H), 4.67, 5.50 (2 m, 1H), 6.80–6.83 (2d, 2H), 6.86 (s, 1H), 7.48–7.59 (m, 3H), 7.83–7.86 (m, 2H), 7.90, 8.13 (2s, 1H), 8.51–8.60 (2d, 1H), 9.88 (s, 1H), 11.17, 11.34, 11.90 (3s, 2H); ESI-MS: *m/z* calcd: 407.16, found: 408.0 [(M+1)⁺].

4.2.23. (S,E)-N-(1-(2-(Furan-2-ylmethylene)hydrazinyl)-3-(1H-imidazol-4-yl)-1-oxopropan-2-yl)-4-methoxybenzamide (8g)

Compound **8g** was white solid, mp 210–211 °C, yield 59.2%. ¹H NMR (DMSO-*d*₆) δ 3.04 (s, 2H), 3.81 (s, 3H), 4.67, 5.45 (2 m, 1H), 6.61–6.64 (m, 1H), 6.87–6.92 (m, 2H), 7.59 (s, 1H), 7.82–7.87 (m, 3H), 7.90, 8.14 (2s, 1H), 8.55–8.63 (2d, 1H), 11.33, 11.51, 11.95 (3s, 2H); ESI-MS: *m/z* calcd: 381.14, found: 382.0 [(M+1)⁺].

4.3. Biological evaluation

Antiviral evaluation: inhibition of SIV-induced syncytium in CEM174 cell cultures was measured in a 96-well microplate containing 1×10^5 CEM cells/mL infected with 100 TCID₅₀ of SIV per well and containing appropriate dilutions of the tested compounds. After 5 days of incubation at 37 °C in 5% CO₂ containing humidified air, CEM giant (syncytium) cell formation was examined microscopically. The EC₅₀ was defined as the compound concentration required to protect cells against the cytopathogenicity of SIV by 50%. TC₅₀ assay was performed in uninfected CEM174 cells under the same condition above, and the value was determined as the concentration required to inhibit CEM cells proliferation by 50% in MTT reduction assay.

Assembly inhibitory assay: ultraviolet spectrophotometry assay was performed at 350 nm on a Agilent 8453 spectrophotometer. A 1.0 μL of concentrated ligand in DMSO (1 mM) was added to a 75 μL aqueous solution, then added 25 μL capsid protein (40 μM) to initiate the reaction. Spectral measurements were made every 10 s, following a short initial delay to allow sample equilibration. Relative assembly rates were estimated from initial slopes of the plots of absorbance versus time.

4.4. Molecular modeling

The initial structure of our compounds were subjected to minimization using MOPAC in Chemoffice 2005 and the 3D structure of HIV-1 capsid in complex with its inhibitor CAP-1 was recovered from the Protein Database with the code as 2JPR.¹⁰ The advanced docking program AUTODOCK 4.0 was used to remove the small molecule and perform the automatic molecular docking with our compounds. The number of generations, energy evaluation, and docking runs were set to 370,000, 1,500,000, and 20, respectively, and the kinds of atomic charges were taken as Kollman-all-atom for macromolecular and Gasteiger–Hücel for the compounds.

Acknowledgment

The project was supported by the National Natural Science Foundation of China (No. 30670415).

References and notes

- Turner, B. G.; Summers, M. F. *J. Mol. Biol.* **1999**, *285*, 1.
- Barbie, K.; Ganser-Pornillos, Cheng, A.; Yeager, M. *Cell* **2007**, *131*, 70.
- Tang, C.; Loeliger, E.; Kinde, I.; Kyere, S.; Mayo, K.; Barklis, E.; Sun, Y.; Huang, M.; Summer, M. F. *J. Mol. Biol.* **2003**, *327*, 1013.
- Tian, B.; He, M.; Tang, S.; Hewlett, I.; Tan, Z.; Li, J.; Jin, Y.; Yang, M. *Bioorg. Med. Chem. Lett.* **2009**, *19*, 2162.
- Li, Y.; Wang, Y.; Jing, K.; Peng, Q.; Liu, S.; Zhang, Z. *Chin. J. Magn. Reson.* **2005**, *22*, 7.
- Pallaa, G.; Predierib, G.; Domiano, P. *Tetrahedron* **1986**, *42*, 3649.
- Lanman, J.; Sexton, J.; Sakalian, M.; Prevelige, P. E. *J. Virol.* **2002**, *76*, 6900.
- West, J. B.; Wong, C. H. *J. Org. Chem.* **1986**, *51*, 2728.
- Prein, M.; Manley, P. J.; Padwa, A. *Tetrahedron* **1997**, *53*, 7777.
- Kelly, B. N.; Kyere, S.; Kinde, I.; Tang, C.; Howard, B. R.; Robinson, H.; Sundquist, W. I.; Summers, M. F.; Hill, C. P. *J. Mo. Biol.* **2007**, *373*, 355.